

Phosphorus speciation in sediments and assessment of nutrient exchange at the water-sediment interface in a Mediterranean lagoon: Implications for management and restoration



Noureddine Zaaboub^a, Anouar Ounis^b, Mohamed Amine Helali^b, Béchir Béjaoui^a, Ana Isabel Lillebø^c, Eduardo Ferreira da Silva^d, Lotfi Aleya^{e,*}

^a Institut National des Sciences et Technologies de la Mer Salammbô, Tunisia

^b Faculté des Sciences de Tunis, Université de Tunis El Manar, Tunisia

^c CESAM-Centre for Environmental and Marine Studies & Department of Biology, University of Aveiro, 3810-193 Aveiro, Portugal

^d Universidade de Aveiro, Departamento de Geociências, GeoBioTec-Goebiociências, Geotecnologias e Geoengenharias, Campus de Santiago, 3810-193 Aveiro, Portugal

^e Laboratoire de Chrono-Environnement, UMR CNRS 6249 Besançon, France

ARTICLE INFO

Article history:

Received 10 March 2014

Received in revised form 29 July 2014

Accepted 2 September 2014

Available online 21 September 2014

Keywords:

Phosphorus

Sequential extraction

Benthic chamber

Coastal lagoon

Sediment composition

ABSTRACT

Bioavailable P-forms in Bizerte lagoon and the adjacent open waters of the north-eastern Mediterranean, were quantified with the SEDEX sequential extraction method. Pore water analysis, sediment total organic carbon and the mineralogical composition of sediment samples were also determined and potential P release at the lagoon's water-sediment interface was assessed through benthic chamber experiments. Sediment shows an abundance of quartz and calcite in different core samples from the lagoon center, while pyrite is observed in samples from the open sea. Relative abundance of Fe-bound phosphorus in the sediments reveals the co-precipitation of both constituents as P-containing iron (oxyhydr) oxides. Phosphorus bioavailability was greater in the lagoon than in the open sea, dependent on Ca–P fractionation, and promoting P sediment immobilization. Pyrite presence is related to periodic anoxic events inducing P release upwards in relation to periodic increases in organic loads.

© 2014 Elsevier B.V. All rights reserved.

1. Introduction

The surface layer of the eastern Mediterranean is mainly comprised of the Atlantic waters arriving from the Atlantic Ocean through the Strait of Gibraltar. The usual nutrient-poor Atlantic Tunisian Current (Ben Ismail et al., 2012, 2014), originating in the Tunisia-Sicily channel, flows along the Tunisian coast to reach different zones, including Bizerte lagoon where increased eutrophication in its water quality is detected (Ben Ameer et al., 2013). Indeed, studies conducted over the years, describing phytoplankton dynamics in relation with nutrient availability in the lagoon water column, have demonstrated the role of anthropogenic nutrients in triggering harmful algal blooms (Sahraoui et al., 2009; Smida et al., 2012; Turki et al., 2014), with the ability of some strains to cause shellfish poisoning (Turki et al., 2014) and/or to form resting cysts which accumulate in the sediments (Fertouna-Bellakhal et al., 2014). Information on the status of phosphorus in

the sediment, on the other hand, is totally lacking. Yet when trapped in sediment, this element may, under precise conditions (Alaoui et al., 1994, 2014; Andrieux-Loyer et al., 2008), be released upwards as a biologically available nutrient that will support phytoplankton growth (Aleya, 1992). Since summer in the lagoon is characterised by low watershed input, with the N/P in the water column higher than the Redfield ratio (16), thus suggesting phosphorus limitation, we hypothesised that phytoplankton growth during the summer hypolimnetic anoxia might be supported by the diffusive fluxes from the water-sediment interface. It was therefore urgent to investigate phosphorus speciation so as to understand the association of sediment bound to P, and to undertake benthic chamber experiments in order to estimate the potential release of phosphorus and thus help to propose management tools to mitigate the lagoon's eutrophication.

In the Mediterranean, many studies have been carried out to investigate fractionation and sorption/desorption of P in surface sediment (Krom et al., 2003, 2010), with the sequential chemical extraction of P selected as the most suitable means to examine these processes (Eijssink et al., 1997; Anderson and Delaney, 2000).

* Corresponding author. Tel.: +33 381 66 57 64; fax: +33 381 66 57 97.
E-mail address: lotfi.aley@univ-fcomte.fr (L. Aleya).

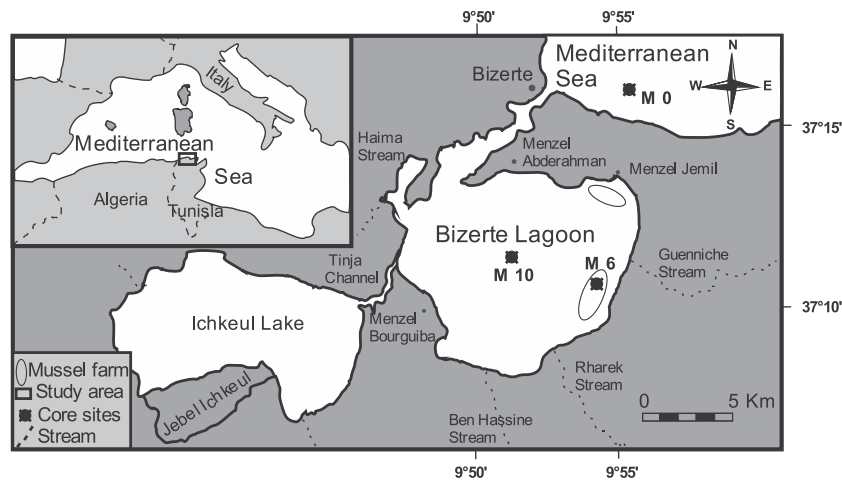


Fig. 1. Geographical position of the studied area in Tunisia and localization of the investigated core sediment in the Mediterranean Sea and Bizerte lagoon.

Phosphorus can be associated with Fe, Ca oxides and Al or be adsorbed on the surface of minerals and organic materials, with salinity, pH or redox potential regulating the relative importance of each fraction (Avilés et al., 2006; Van der Heide et al., 2010). However, no such information is available for the north-eastern Mediterranean.

This study aims to (a) improve our understanding of P fractionation in core sediment samples, (b) determine the proportion of available phosphorus fractions and (c) evaluate their possible contributions to P release in Bizerte lagoon, especially during periods of hypolimnetic anoxia.

2. Materials and methods

2.1. Study site

Bizerte lagoon in northern Tunisia is connected to the Mediterranean Sea from its eastern shore by a narrow (300 m wide) channel. Connected to Ichkeul Lake from its western shore by a channel approximately 5 km long (Fig. 1), the lagoon has a surface area of 121.6 km² and maximum and mean depths of 12 and 8 m. Salinity in the lagoon ranges from 33 to 35 p.s.u, whereas in the inlet it is similar to that of sea (36 p.s.u). The total amount of fresh water discharged into the lagoon is 125 Mm³ y⁻¹. The lagoon's environment is threatened by anthropic interferences, yet a large mussel farm operates there, mainly in the eastern zone (Fig. 1). In addition to marine and continental influences, the lagoon is affected by urban and industrial effluents. The southern part of the lagoon contains an iron factory and a shipyard, but the northern part, receiving abundant industrial waste, is the part most affected by human activities.

2.2. Sampling and processing

Three core samples were manually retrieved from the bottom of the lagoon by scuba divers: an open sea core at 22 m depth opposite the city of Bizerte (Core M0: marine station) and two cores inside the lagoon (Cores M6 and M10, at 8 m and 12 m depth, respectively) (Fig. 1). Samples were collected by inserting 60 cm long polyethylene tubes with a 9 cm diameter into the sediment. The collected core sediments were opened immediately under strict anoxic conditions in a nitrogen-filled glove box to prevent oxidation. The subsamples were transferred under N₂ atmosphere into centrifugation tubes for pore-water extraction through centrifuging for 30 min at 3000 rpm. The supernatant pore water was filtered, under an N₂ atmosphere, using a Minisart[®] NML

syringe filter with 0.45 μm pore size, then placed in clean sample bottles and frozen at -20 °C. Sediment subsamples were then also stored at -20 °C.

2.2.1. X-ray diffractometer (XRD) analysis and scanning electron microscopy (SEM) observation

Mineralogical analyses were carried out by means of a PANalytical X'Pert PRO (XRD). The different mineral phases were evaluated with the X'pert HighScoreplus[®] programme. Pyrite was observed by means of an ESEM Type JEOL JSM -5400 scanning microscope.

2.2.2. Phosphorus fractionation

To understand the cycling of P in the Mediterranean and its effect on present times, greater insight into this element's behavior in western Mediterranean sediments is crucial. Ruttenberg (1992) published a sequential extraction technique for marine sedimentary phosphorus (the SEDEX method) which, according to Eijssink et al. (1997), applies to Mediterranean sediments. In order to estimate the amount of bioavailable P, five major forms of solid-phase P in sediments were determined using the SEDEX procedure (Ruttenberg, 1992; Akhurst et al., 2004):

- 1) Exchangeable or loosely bound labile P (lab-P) using MgCl₂ as an extractant,
- 2) Ferric-bound (oxide associated) P (Fe-P) using citrate-dithionite-bicarbonate (CDB) solution,
- 3) Calcium carbonate associated P, authigenic carbonate fluorapatite and biogenic apatite (Ca-P) extracted with 1 M sodium acetate buffered to pH of 4.0 using acetic acid,
- 4) Detrital apatite P of igneous or metamorphic origin (detr-P) using HCl dissolution at a low pH and
- 5) Organic P (org-P) using dry oxidation at 550 °C and residue dissolution with HCl dissolution at a low pH.

Steps 2 and 3 are comprised of sub-steps consisting of MgCl and water washes, which prevent dissolved P from readsorption on sediment surfaces. In addition, in step 3, due to high CaCO₃ contents recorded in Mediterranean sediments (more than 60%, this percentage being higher than in other areas such as the North Atlantic), we allowed for additional shaking time as proposed by Eijssink et al. (1997). Phosphorus was analyzed by spectrophotometry using the standard phosphomolybdate blue method (Koroleff, 1976) which cannot, however, be used directly for the CDB solutions since its extractant interferes with the molybdate blue reagent. These solutions were first reacted with a 1% v/v FeCl

Table 1
Eh (mV), TOC values (%) and vertical P concentrations ($\mu\text{mol P/g}$ dried sediment) using SEDEX.

	Core	Depth(cm)	Eh	TOC	lab-P	SD	Fe-P	Ca-P	SD	Detr-P	SD	Org-P	SD	Σ -P
Bizerte lagoon	M6	0–2	–10	1.00	0.60	0.01	0.49	15.02	1.63	0.02	0.09	0.34	0.06	16.47
		2–4	–84	1.12	0.65	0.01	1.49	21.53	0.1	0.01	0.06	0.08	0.15	23.77
		4–6	–100	2.65	0.61	0.04	2.97	21.13	2.41	0.02	0.05	0.68	0.15	25.41
		6–10	–76	3.21	0.75	0.01	2.34	11.48	1.97	0.02	0.04	0.07	0.02	14.66
		10–16	–84	0.89	0.73	0.01	4.07	19.37	0.87	0.00	0.03	0.15	0.02	24.33
	M10	16–20	–68	1.09	0.68	0.04	1.55	15.91	0.37	0.02	0.09	0.06	0.04	18.22
		0–2	10	1.22	0.77	0.01	2.49	15.91	0.87	0.29	0.01	0.37	0.02	19.84
		2–4	–40	1.13	0.80	0.01	3.76	12.42	0.57	0.33	0.06	0.27	0.55	17.58
		4–6	–45	1.10	0.78	0.04	3.34	14.71	2.29	0.07	0.02	2.46	0.37	21.35
		6–8	–98	1.07	0.60	0.01	3.97	23.87	0.03	0.16	0.03	0.98	0.08	29.58
		8–10	–120	0.99	0.64	0.01	4.92	23.98	1.46	0.05	0.05	1.30	0.22	30.89
		10–12	–100	0.96	0.61	0.03	5.71	18.15	2.21	0.04	0.09	0.42	0.14	24.93
		12–14	–98	1.17	0.48	0.04	5.02	10.15	2.44	0.04	0.01	1.00	0.14	16.70
		14–16	–90	1.41	0.47	0.01	2.81	19.89	2.21	0.00	0.04	0.45	0.23	23.63
		16–18	–78	1.55	0.42	0.06	3.92	11.04	0.22	0.01	0.08	1.37	0.32	16.76
		18–22	–69	1.39	0.42	0.01	2.18	10.15	0.55	0.01	0.05	0.10	0.01	12.87
		22–28	–97	1.41	0.37	0.01	5.07	12.37	0.55	0.00	0.04	0.08	0.08	17.90
		28–33	–84	1.43	0.41	0.01	2.34	14.58	0.54	0.00	0.01	0.07	0.01	17.39
		33–37	–62	1.57	0.45	0.03	2.97	14.58	0.24	0.03	0.09	0.01	0.07	18.04
Open sea	M0	0–5	25	2.32	0.42	0.04	1.86	12.13	0.45	0.03	0.07	0.02	0.14	14.47
		5–10	10	1.36	0.37	0.06	3.18	5.72	0.24	0.03	0.08	0.66	0.08	9.97
		10–16	–115	2.28	0.34	0.01	2.92	11.48	2.41	0.04	0.03	1.55	0.02	16.32
		16–20	–135	1.88	0.33	0.07	2.28	3.59	1.63	0.04	0.01	0.18	0.09	6.42
		20–24	–100	1.97	0.21	0.08	2.71	12.81	0.17	0.03	0.04	0.03	0.07	15.79

solution (Lucotte and D'Anglejan, 1985) extracted into isobutanol and then analyzed by spectrophotometry (Watanabe and Olsen, 1962; Ruttenberg, 1992). Finally, each extraction step is individually standardized to ensure extractant selectivity and specificity. Details of extraction methods are completed by several sample analyses in triplicate that permit precision in techniques based on standard deviation of results (Table 1).

2.2.3. Total organic carbon (TOC)

This was determined in sediment samples by means of a PerkinElmer PE 2400CHN. The subsamples for TOC analysis were de-carbonated using 1 M HCl and dried at 60 °C.

2.2.4. Pore-water analysis

The sediment core was handled under N_2 atmosphere. In the M6 core sediment the supernatant pore water was filtered under N_2 atmosphere, onto a membrane with a pore size of 0.45 μm to determine concentrations of PO_4^{3-} , Mn and Fe using a flame atomic absorption spectrophotometer (SOLAAR). At least one

duplicate was run for every 2 samples to verify precision which, proved to be approximately 10%.

2.2.5. Benthic chamber experiments

Our benthic chambers were transparent box-shaped acrylic containers (length (L)=0.2 m, surface (S)=0.25 m^2 , volume (V)=0.05 m^3) with plastic lids above the chamber attached by four stainless steel clips. The lid contained a sampling port with a syringe holder for water samples (Fig. 2). The water inside the chambers was stirred by a flat rotating disk (15 cm diameter) connected to a DC motor with gear box. The rpm of the stirring disk were adjusted and controlled electronically (Fig. 2). Synergy collected 50 ml of water every 2 h 30 min. Thus, over 24-h periods, 9 samples were automatically taken. Samples collected from the device were immediately filtered through a 0.45 μm pore size filter, while pH, Eh and O_2 were measured immediately upon removal from the chamber. Ammonium, nitrate, nitrite, phosphate sulfate and silicate were analyzed via techniques using a “Technicon III” colorimetric auto-analyzer.

2.3. Statistical analysis

Statistics were analyzed with the SPSS program to detect potential correlations between Mn and Fe in pore water from the M6 core sediment and phosphorus fractions.

3. Results

3.1. XRD and SEM observation

The sediments of the outlet of Bizerte Lagoon are mainly silty-clays with alternating gray and dark gray layers. According to the XRD results (Figs. 3 and 4) the sediments are dominated by quartz and calcite, with pyrite also present in some samples. In the inner part of the lagoon the same composition is found, but with a higher phyllosilicate percentage.

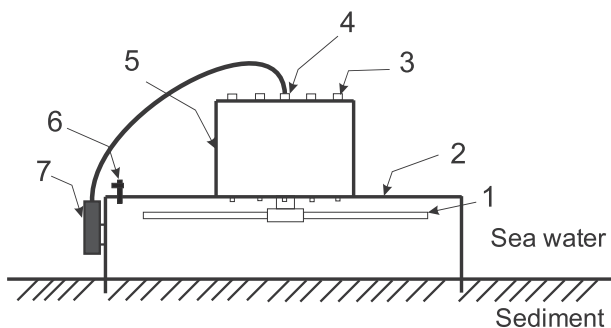


Fig. 2. Transparent benthic chamber, (1) stirrer; (2) PVC bottom; (3) sampling syringe; (4) pressure control syringe; (5) motor chamber; (6) control valve; (7) battery.

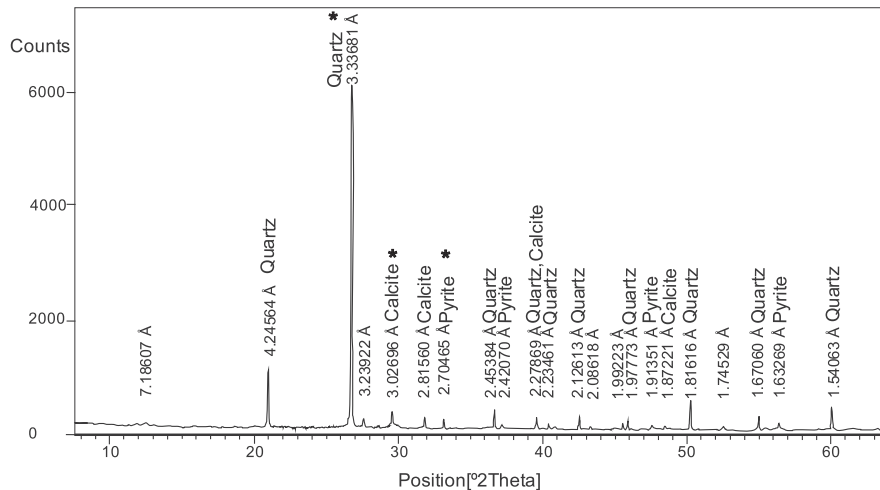


Fig. 3. X-ray diffractogram of M0 (10–16 cm) sediment. Peaks marked with an asterisk (*) represent the highest peak of intensity for each mineral. No matched peaks represent very minor phases which cannot be identified with XRD.

Pyrite is present in the core sediments from both the lagoon center and the outlet. In the marine core sediment quartz is dominant with a median value of 81%, its median percentage being 39%, followed by phyllosilicates with 29% (median value). Presence of pyrite and aragonite is also observed, but at a lower percentage (Fig. 4). Examination of pyrite morphology with SEM in samples from the lagoon center (M10) and open sea (M0), reveals both framboidal and euhedral pyrite, with the framboidal pyrite in M0 presenting irregular forms (Fig. 5).

3.2. Phosphorus speciation in core sediments

Concentrations of phosphorus fractionation (lab-P, Fe-P, org-P and Ca-P) range between 0.4–0.8, 2.2–5.7, 0–2.5 and 10.1–24 $\mu\text{mol P g}^{-1}$, respectively. The depth profiles of the three sampled stations show differences both in number and proportion of P pools with wide prevalence of Ca-P (Fig. 6). In surface core sediment, total phosphorus ranges from 15 to 20 $\mu\text{mol P g}^{-1}$. As depth increases,

higher levels of P concentration alternate with lower ones, apparently according to site.

3.3. TOC distribution

The TOC results show a mean value of 1.66% in open sea sediment samples and 1.39% in the Bizerte lagoon core sediment (Table 1) which presents a homogenous repartition with presence of enriched TOC in some layers (Table 1).

3.4. Interstitial water analysis for (M6) core sediment

Mussel farms, having direct influence over sediments, are important sites for the study of biogeochemical processes, with interstitial water analysis providing additional information.

The Eh values vary from –10 to –100 mV as shown in Table 1 and the pH from 7.8 to 8.5. The concentrations of Fe and Mn in the pore water of reduced muddy sediments were analyzed (Table 2),

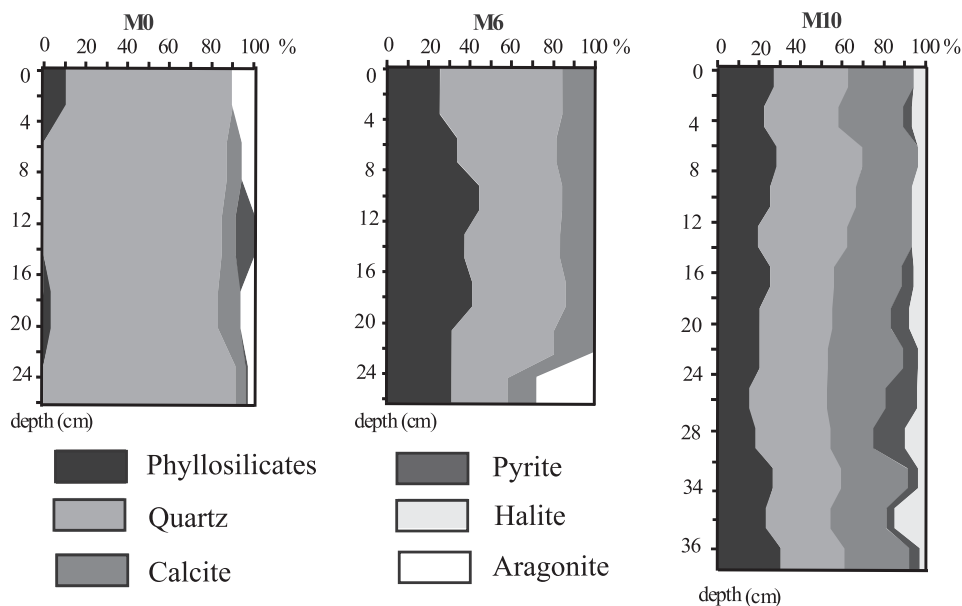


Fig. 4. Percentage of minerals in core sediments (semi quantitative results).

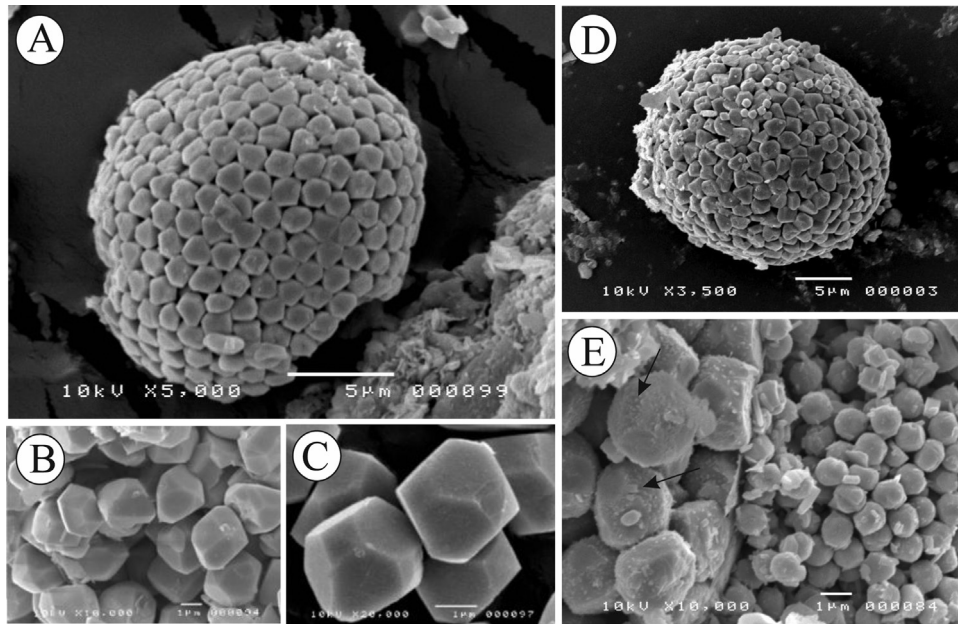


Fig. 5. (A) frambooidal pyrite from deeper M10 core sediment; (B) euhedral pyrite in lagoon sediment; (C) detail of euhedral pyrite of the investigated M10 core sediment; (D) frambooidal pyrite from M0 core sediment in open sea; (E) detail of frambooidal pyrite from M0 core showing irregular forms on surface (indicated by arrows).

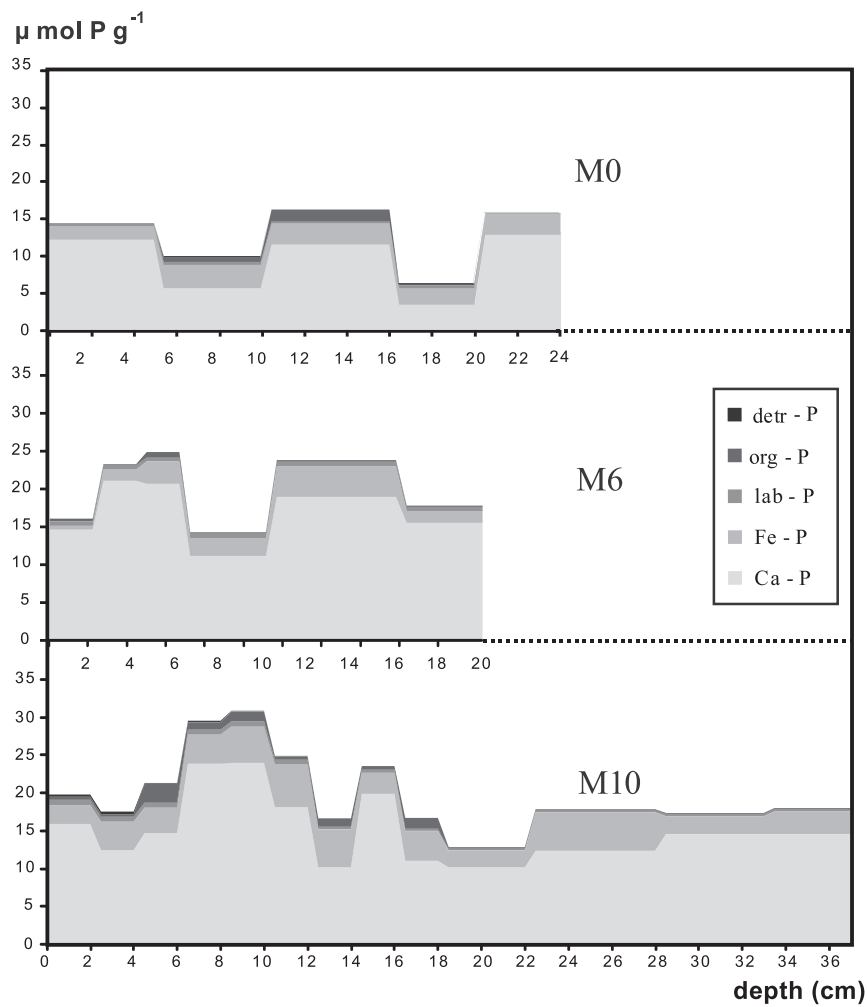


Fig. 6. Phosphorous fractions profiles in different core sediment.

Table 2
Values of pH, Eh, Mn and Fe recorded in the interstitial water of M6 core sediment.

Core	Depths cm	pH	Eh mV	Mn $\mu\text{g l}^{-1}$	Fe mg l^{-1}	
Bizerte lagoon	M6	0–2	7.8	–10	323	1224
		2–4	7.9	–84	237	1172
		4–6	8	–100	164	1278
		6–10	8	–76	98	1325
		10–16	8.3	–84	31	1041
		16–20	8.5	–68	72	1133

showing mean concentrations of 1196 mg l^{-1} and $154 \mu\text{g l}^{-1}$, respectively. In the M6 core sediment, NO_3^- and PO_4^{3-} exhibited average values of $2.51 \mu\text{mol l}^{-1}$ and $0.51 \mu\text{mol l}^{-1}$ (Table 3), respectively.

3.5. Benthic flux

Flux chamber data are summarized in Table 4. It is noteworthy that the chamber was installed in sediment on the eastern side of the lagoon, characterized by suboxic to anoxic conditions so as to detect potential nutrient fluxes. Globally, waters in the benthic chamber remain oxic throughout the incubation experiment; the concentration (0.18 in $0.15 \mu\text{M}$) remains far from the limit at which the concentration in O_2 stabilizes ($\sim 0.6 \mu\text{M}$). The contents in NH_4^+ vary from 7.30 to $14.09 \mu\text{M}$ with increasing evolution during incubation. The amount of PO_4^{3-} varies from 0.11 to 0.38. Silica concentration in the chamber ranges from 1.32 to $2.03 \mu\text{M}$. Observation of NO_2^- and NO_3^- variation shows a progressively decreasing trend from the beginning to the end of the experiment.

3.6. Correlations

Correlation between Mn and Fe in the M6 core sediment, along with other parameters show a significant correlation with phosphorus fraction associated to iron (Fe–P). The correlation with Mn is significant ($r = -0.75$, $p < 0.05$), but with Fe it becomes more significant ($r = -0.97$, $p < 0.05$) when samples taken out of Fe–P accumulation zones are included in the analysis. Significant correlation was observed between Fe and PO_4^{3-} ($r = -0.90$, $p < 0.05$).

4. Discussion

4.1. Phosphorus speciation in core sediments and pyrite formation

P fractions in different core sediments show dominance of calcium-bound P deposits (Ca–P) (Table 1 and Fig. 6). In lagoons and other marine environments, CaCO_3 is produced at high salinity rates through precipitation reactions and biological activity, forming an adsorption substrate for dissolved phosphate (Avilés et al., 2006; Van der Heide et al., 2010). In northern Tunisia, Ca-bound P is the major phosphorus form in marine sediments, associated mainly with the oversaturation of calcite and

Table 4
pH, O_2 and nutrient concentrations recorded during benthic chamber incubation.

Time (h)	4.5	6.75	9	11.25	13.5	15.75	18
pH	8.30	8.27	8.25	8.25	8.23	8.20	8.19
$\text{O}_2 \text{ mmol l}^{-1}$	0.16	0.17	0.17	0.14	0.16	0.17	0.16
$\text{NO}_2^- \text{ mmol l}^{-1}$	1.35	0.67	0.64	0.59	0.65	0.61	0.59
$\text{NH}_4^+ \text{ mmol l}^{-1}$	7.31	8.12	9.46	11.39	11.16	12.3	14.1
$\text{NO}_3^- \text{ mmol l}^{-1}$	5.20	2.70	4.42	2.90	2.42	2.21	2.75
$\text{PO}_4^{3-} \text{ mmol l}^{-1}$	1.25	0.39	0.13	0.33	0.33	0.11	0.14
Silicates mmol l^{-1}	1.32	1.53	1.55	1.52	2.03	1.99	1.70
$\text{SO}_4^{2-} \text{ g l}^{-1}$	1.44	1.15	0.91	0.82	0.67	0.48	0.72

co-precipitation of phosphate. Moreover, the calcareous nature of the lagoon watershed has certainly contributed to CaCO_3 enrichment.

The general shapes of Fe–P concentration profiles are similar at all three sites indicating an accumulation between 5 and 10 cm depth along core sediment profiles (Fig. 7). In this area, phosphate and ferrous iron diffuse in both directions, upwards to the surface layer and downwards into deeper sediments. This affinity between Fe and P is confirmed by a significant correlation between Fe and PO_4^{3-} in the interstitial water ($r = -0.90$, $p < 0.05$). It was indeed shown that within the oxic zone ferrous iron is re-oxidized and forms iron (oxyhydr) oxides which offer ideal new surfaces for the (re) adsorption of pore water phosphate (Kuster-Heins et al., 2010). In our study, this co-precipitation is expressed by the concentrations of particulate P–Fe extracted during P sequential extraction with CDB (Fig. 7). These results are in accordance with previous studies which suggest a sink for P just below the iron reduction zone (Zabel et al., 1998). Low values of labile P occurred in surface layers and even decreased with depth to lower values in core sediment at mussel farms. These results are in agreement with observations made in other estuarine systems (Thouvenot-Korppoo et al., 2012) where labile fractions are limited, while more refractory pools dominated in deeper sediments. The organic matter-rich layer observed mainly in our open sea core sediment samples, in presence of low potential redox, may indicate the preservation of organic matter and promotes the formation of pyrite (Tang and Stott, 1993).

The mussel farm core sediment (M6) was taken in the lagoon's eastern sector, where water movement is weak, sediment is suboxic to anoxic and phytoplankton abundant (Turki et al., 2014). As the reactivity of Fe-bound P was assumed to depend on redox potential and pH (Gomez et al., 1999; Alaoui et al., 2014), we measured the iron concentration in the interstitial water (Table 2). The results point to a significant negative correlation ($r = -0.819$, $p < 0.05$) between Mn in pore water and Fe–P. However, no significant correlation between Fe in pore water and Fe–P was found ($r = -0.042$, $p > 0.05$), possibly explained by the peak in iron accumulation as illustrated in Fig. 7. Indeed, when we eliminate the peak value, we obtained a highly significant negative correlation between Fe in pore water and Fe–P ($r = -0.988$, $p < 0.05$). These results suggest an equilibrium between Fe, Mn in pore water and Fe–P. However, the examination of pore water profiles of Fe and Mn and the Fe–P concentration profiles indicate an additional

Table 3
Nutrient concentrations recorded in the interstitial water of M6 core sediment.

Core	Depths cm	PO_4^{3-} $\mu\text{mol l}^{-1}$	NO_2^- $\mu\text{mol l}^{-1}$	NO_3^- $\mu\text{mol l}^{-1}$	NH_4^+ $\mu\text{mol l}^{-1}$	Silicates $\mu\text{mol l}^{-1}$	
Bizerte lagoon	M6	0–2	0.515	0.281	2.456	4.954	1.639
		2–4	0.495	0.903	2.598	10.271	0.360
		4–6	0.493	0.153	2.313	6.926	2.479
		6–10	0.450	0.993	1.113	14.486	2.280
		10–16	0.611	0.036	1.780	9.785	2.182
		16–20	0.520	0.142	1.324	6.190	2.160

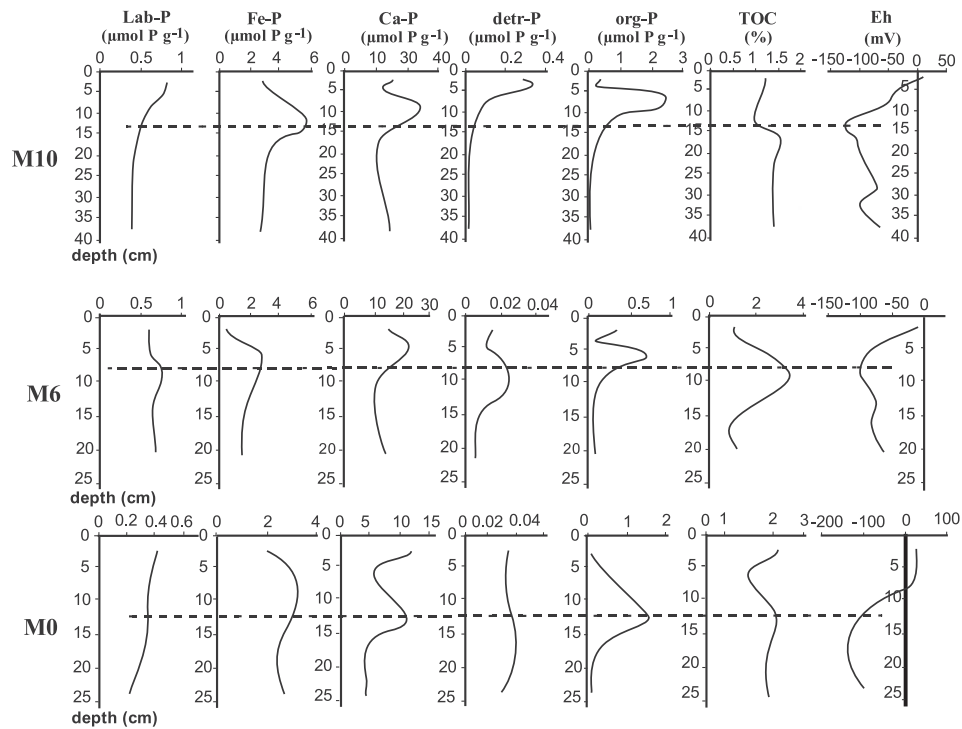


Fig. 7. Fractionation of P concentration and TOC percentage in sediment samples of the different cores examined in this study. (Dash lines: correspond to organic matter accumulation zone; phosphate may have been released both by organic matter degradation and by reductive dissolution of iron and manganese oxyhydroxides. In the upper and more oxygenated layer phosphate will be associated with iron and form Fe–P pic as shown in the figure.)

diagenetic source. This affinity between Fe (oxyhydr) oxides in pore water and phosphate is supported by the correlation between Fe and PO_4^{3-} in M10 cores sediment pore water ($r = -0.90$, $p < 0.05$) and other observations showing strong adsorption of iron to P (Nowacka and Stone, 2006). It has also been shown that the adsorption of P in pore water is closely associated with the redox-sensitive behavior of Fe, at least under the oxic to suboxic conditions (Poulton and Canfield, 2006; Kuster-Heins et al., 2010) which are obviously present in the eastern section of Bizerte lagoon. The relationship between Fe–P and ferrous iron concentration profiles indicates a balance between the two components at

the same depth intervals. In both the lower and surface layer cores in the central part of Bizerte lagoon (M10), as well as in the open sea (M0) core, the pyrite formation in sediment is well developed. Both euhedric and framboidal pyrite were distinguished, the latter with similar grain size distribution which may indicate that its formation occurred predominantly at the oxic-anoxic transition in this sediment as reported elsewhere (Aragon and Miguens, 2001).

The potential redox recorded in the study area confirms our hypothesis (Table 2), thus the sedimentary P in the lagoon core sediment may be a good indicator of nutrient dynamics, redox conditions and productivity. Since P sediment fractions in the

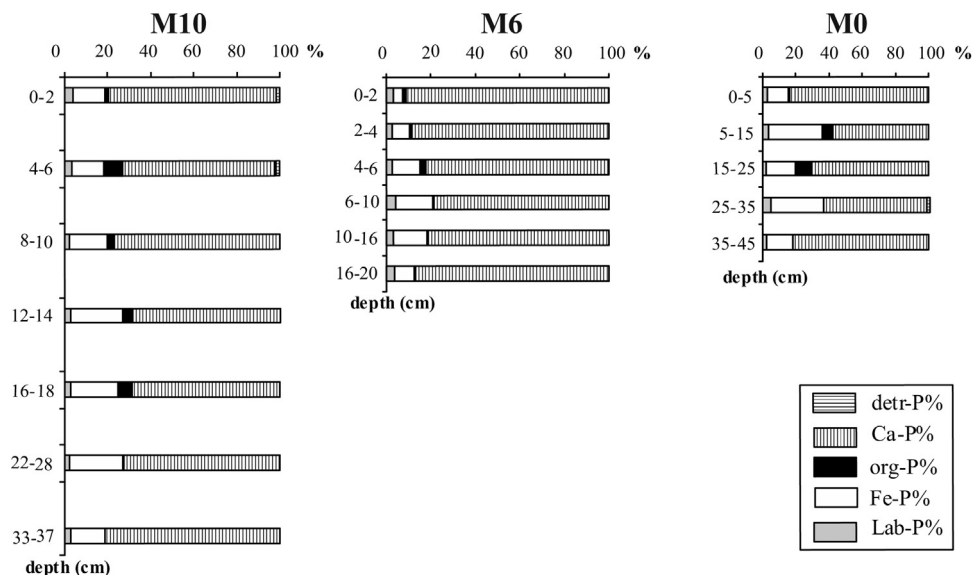


Fig. 8. Phosphorus bioavailability in different core sediments.

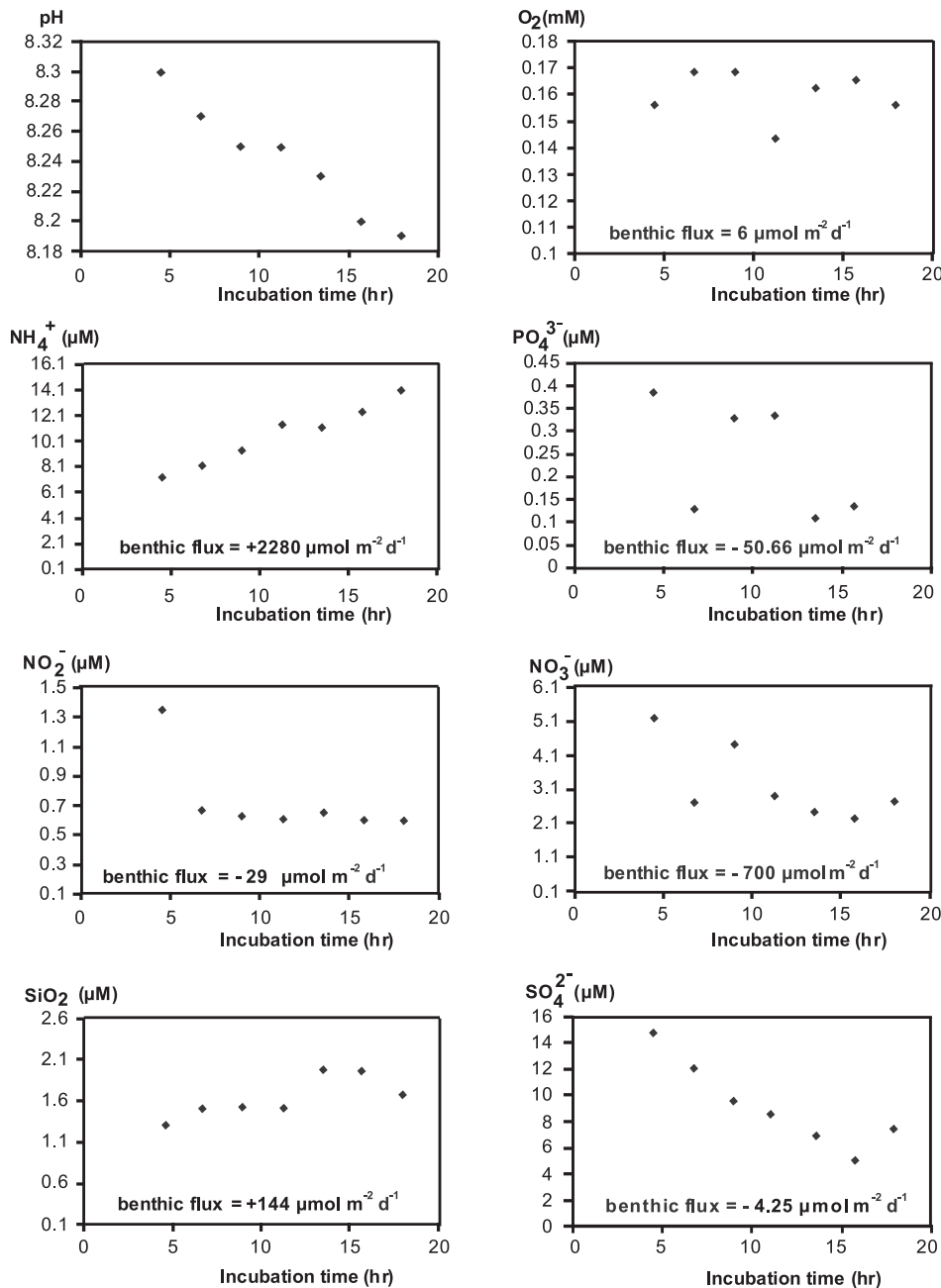


Fig. 9. Benthic flux O_2 and nutrient in eastern area (M6).

Mediterranean exhibit changes in environmental conditions and sediment chemistry (Jilbert et al., 2010; Kraal et al., 2010), our results report more Ca-P in the lagoon than in the open sea (Table 1), which may be explained by the low depth and proximity of lagoon sediment to the continent (Eijsink et al., 2000). Also, differences are observed in phosphorus sediment fractions between the eastern and western Mediterranean, mainly in Ca-P composition. Phosphorus fractions are found in almost the same concentration for different fractions with a small variation for Ca-P, possibly due to depth variations in sample profiles. Indeed, the increase in total P, particularly in shallower water, is mainly due to an increase in Ca-P. In the eastern Mediterranean Sea an increase in total P in surface sediment is observed in the shallow water of the Ionian and Levantine Basins, 16.3 and 23.4 $\mu\text{mol P g}^{-1}$, respectively (Eijsink et al., 2000).

4.2. Phosphorus bioavailability

Considering the five phosphorus fractions, both authigenic and detrital P are almost insoluble under the physico-chemical conditions of estuarine and coastal waters (Andrieux-Loyer et al., 2008) while lab-P, Fe-P and org-P are considered as bioavailable P fractions, i.e., available to photosynthesising plankton. The mean percentage of bioavailable phosphorus is about 21% in the lagoon while it is approximately 16% in the Mediterranean Sea (Fig. 8). Bioavailable P is related to the thickness of the sedimentary layer as it is probably subjected to bioturbation or resuspension. For instance, in Bizerte lagoon, hydrodynamics have an effect on resuspension, from the surface sediment to the water column, to obtain the bioavailable P (Fe-P + org-P + lab-P) within a sedimentary layer of 3 cm (Béjaoui, 2009) where a plethora of dinocysts has been recorded (Fertouna-Bellakhal et al., 2014). Previous studies of P speciation in France have shown that

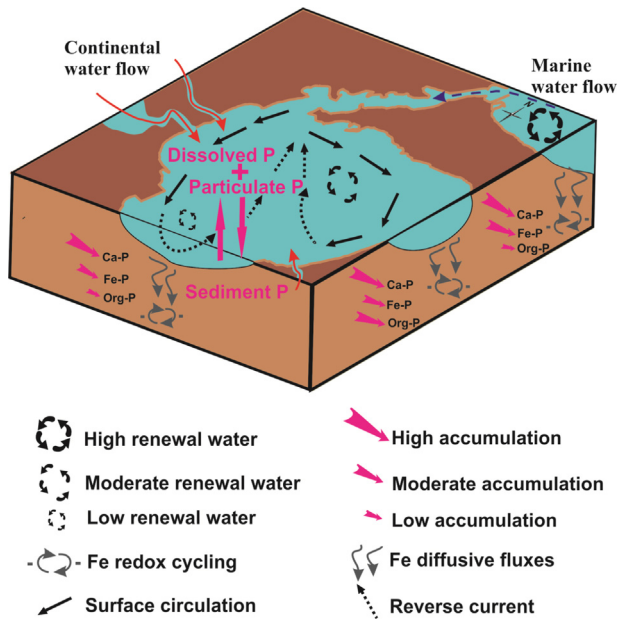


Fig. 10. Phosphorus cycle in Bizerte lagoon during winter.

heavy loads of particles expelled from the Seine estuary during spring floods, contain 50% of bioavailable P and may therefore significantly contribute to the enrichment of phosphorus in the water column (Aminot et al., 1993).

4.3. Phosphorus flux in water sediment interface

The NH_4^+ flux was high in our transparent chamber in winter, $+2280 \mu\text{mol m}^{-2} \text{day}^{-1}$ (Fig. 9), probably the result of increased input in organic debris in the sediments, associated with mussel farm activity. Concerning PO_4^{3-} , the day/night chamber experiments yielded a flux around $-50.6 \mu\text{mole m}^{-2} \text{day}^{-1}$, highlighting

sediment's role as an effective trap for PO_4^{3-} . However, if we consider only night incubation, the benthic flux became positive, averaging $+150 \mu\text{mol m}^{-2} \text{day}^{-1}$ thus suggesting that a fraction of PO_4^{3-} is released upwards into the water column. Yet the PO_4^{3-} increase is not constant during incubation due to the association of phosphates by co-precipitation or by adsorption of this element with the mineral particles, mainly carbonates, as confirmed with the high amount of Ca-P. According to Paytan and Mc Laughlin (2007), desorbed phosphate in oxic sediments is rapidly (re) adsorbed by iron oxyhydroxides or precipitated as Ca-P (Krom and Berner, 1980). In anoxic settings, as confirmed in Bizerte lagoon in summer, the P regenerated from the sediment diffuses upwards into the water column mainly for Lab-P, Fe-P and org-P. Concerning Ca-P, as there is a low amount of CaCO_3 in sediment in this eastern area (~16% in sediment water interface), in anoxic conditions Ca-P may be dissociated and PO_4^{3-} may be desorbed in the water column giving a real boost to phytoplankton development (Aleya, 1992; Slomp, 2011; Alaoui et al., 2014). The PO_4^{3-} in interstitial water is related to pH and the associated alkalinity that reflect the distribution of non-conservative ions in the solution, i.e., distribution between carbonate species. If sufficient calcium is present, microbial metabolisms that induce an increase in alkalinity will cause the equilibrium to shift towards calcium carbonate precipitation, whereas metabolisms that consume alkalinity will result in calcium carbonate dissolution (Baumgartner et al., 2006). In contrast, Lucas and Prévôt (1984) suggest that microorganisms (e.g., bacteria, algae, fungi) releasing PO_4^{3-} ions and making the interstitial water acidic will lead to the dissolution of carbonates. Besides chemical alteration, physical distortion of the mineral lattice by fungal hyphae also potentially plays a role in initiating mineral dissolution (Bonneville et al., 2009). Fig. 10 shows a synthetic illustration of the phosphorus cycle, with low water renewal time, observed in Bizerte lagoon's eastern zone (Bejaoui, 2009). The lagoon's water mass requires several months to completely renew, thus permitting additional Ca-P accumulation in winter when P from the principal water flow at S1 is injected into the lagoon in the form of dissolved and particulate P (Figs. 10 and 11).

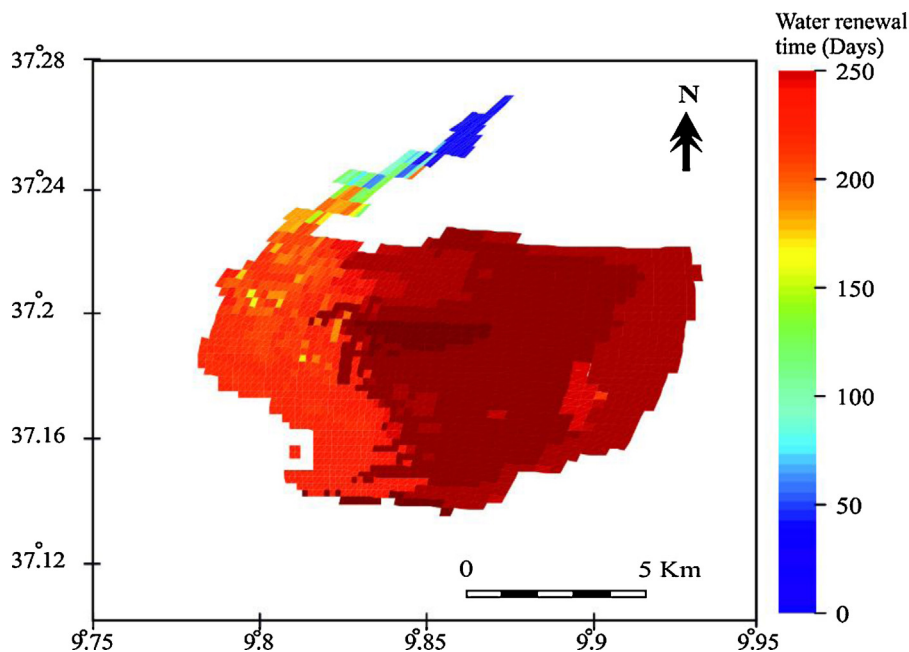


Fig. 11. Water renewal time (WRT) in Bizerte lagoon.

A high organic matter sedimentation rate is produced in the mussel farming area in comparison to the lagoon's central zone leading to low degradation of organic matter and low org-P in the western zone (Fig. 10). The abundant hydrodynamic activity at the lagoon's outlet (Mediterranean Sea) thus gives rise to an area with a higher level of oxicity and redox activity and with greater Fe-P accumulation. This situation is more complex in summer, the anoxic condition resulting in Fe-P dissociation and an upward release of phosphorus, favored by the low renewal water mass found mainly in the eastern area. In addition, the appearance of a reverse current (Fig. 10) in the eastern zone may affect surface sediment causing suspension of sediment particles in this area and remobilization of most bioavailable forms of phosphorus as a labile fraction.

5. Conclusion

A lower total phosphorus level is found in the outlet area than in Bizerte lagoon, which may be related to mineralization factors and the hydrodynamic process. Phosphorus in the lagoon is mainly linked to Ca-P fraction and Fe-P. The amount of Ca-P and Fe-P in sediment also depends on the physical and chemical parameters of sediment, which shows strong interdependence in the cycling of these elements in the marine environment. The CaCO_3 may be considered an important pool in P dynamics. In oxic conditions (winter) sediment is a good immobilizer for phosphorus mainly precipitated as Ca-P, Fe-P and org-P, but in anoxic conditions (summer) the dissolution of Fe-P, org-P and Ca-P at low CaCO_3 content in the sediment area may be observed, mainly in the lagoon's eastern zone. This PO_4^{3-} may reach the water column and thus seriously boost phytoplankton development with harmful algal bloom sequences. A high level of diagenetic interaction is reached between (sub) oxic and anoxic sediment layers favoring pyrite formation and development of eutrophic conditions.

The sediment in Bizerte lagoon is a time bomb, due to (1) phosphorus release at the water-sediment interface and (2) accumulation of toxic dinocysts and the appearance of time windows for their germination (Fertouna-Bellakhal et al., 2014), both exacerbated by the increased aquaculture in the lagoon's coastal waters and other sources of eutrophication (Béjaoui-Omri et al., 2014). Remediation measures are urgently required to limit the extent of the problem. We do not believe that dredging is a suitable solution since it cannot improve water circulation in the lagoon (Béjaoui et al., 2008; Béjaoui, 2009). In addition, dredging may have a serious geochemical impact: trace elements that have been trapped with the acid volatile sulphide may be released thus affecting the biota. Another possible managerial operation may be one recently suggested by D'Errico et al. (2013), bioremediation consisting of stimulating the degradation of the high organic load in Bizerte lagoon sediments through introduction of compost.

Acknowledgments

This work is part of a collaborative project between the INSTM (Institut National des Sciences et Technologie de la Mer Tunisia), the University of Franche-Comté (Chrono-Environnement, UMR CNRS 4269, Besançon, France) and the University of Aveiro, Portugal.

References

Akhurst, D., Jones, G.B., Mc Conchie, D.M., 2004. The application of sediment capping agents on phosphorus speciation and mobility in a sub-tropical dunal lake. *Mar. Freshwater Res.* 55, 715–725.

Alaoui, M.M., Aleya, L., Devaux, J., 1994. Phosphorus exchanges between sediment and water in trophically different reservoirs. *Water Res.* 28, 1971–1980.

Alaoui, M., Dhib, M., Bouhaddiou, A., Ziadi, A., Turki, B., Aleya, S., 2014. Assessment of nitrogen and phosphate balance and the roles of bacteria and viruses at the water-sediment interface in the Allal El Fassi reservoir (Morocco). *Environ. Monit. Assess.* 186, 5817–5829.

Aleya, L., 1992. The seasonal succession of phytoplankton in a eutrophic lake through the coupling of biochemical composition of particulates metabolic parameters and environmental conditions. *Archiv für Hydrobiologie* 124, 69–88.

Aminot, A., Guillaud, J.F., Andrieux, F., 1993. Spéciation du phosphore et apports en Baie de Seine orientale. *Oceanol. Acta* 16, 617–623.

Anderson, L.D., Delaney, M.L., 2000. Sequential extraction and analysis of phosphorus in marine sediments: streamlining of the SEDEX procedure. *Limnol. Oceanogr.* 45, 509–515.

Andrieux-Loyer, F., Philippon, X., Bally, G., Kérouel, R., Youenou, A., Le Grand, J., 2008. Phosphorus dynamics and bioavailability in sediments of the Penzé Estuary (NW France): in relation to annual P-fluxes and occurrences of *Alexandrium Minutum*. *Biogeochemistry* 88, 213–231.

Aragon, G., Miguens, F., 2001. Microscopic analysis of pyrite in the sediments of two Brazilian mangrove ecosystems. *Geo. Mar. Lett.* 21, 157–161.

Avilés, A., Rodero, J., Amores, V., Vicente, I., Rodríguez, M.L., Niell, F.X., 2006. Factors controlling phosphorus speciation in a Mediterranean basin (River Guadalfeo Spain). *J. Hydrol.* 331, 396–408.

Baumgartner, L.K., Reid, R.P., Dupraz, C., Decho, A.W., Buckley, D.H., Spear, J.R., Przekop, K.M., Visscher, P.T., 2006. Sulfate reducing bacteria in microbial mats: changing paradigms new discoveries. *Sediment. Geol.* 185, 131–145.

Béjaoui, B., Harzallah, A., Moussa, M., Chapelle, A., Solidoro, C., 2008. Analysis of hydrobiological pattern in the Bizerte lagoon (Tunisia). *Estuar. Coast. Shelf Sci.* 80, 121–129.

Béjaoui, B., 2009. Développement d'un Modèle Tridimensionnel Couplé Dynamique-Ecologie: Application à la Lagune de Bizerte. PhD thesis. Ecole Nationale des Ingénieurs de Tunis, Tunisia, 250p.

Béjaoui-Omri, A., Béjaoui, B., Harzallah, A., Aloui-Béjaoui, N., El Bour, M., Aleya, L., 2014. Dynamic Energy Budget Model: a monitoring tool for growth and reproduction performance of *Mytilus Galloprovincialis* in Bizerte Lagoon (Southwestern Mediterranean Sea). *Environ. Sci. Pollut. Res.* doi:http://dx.doi.org/10.1007/s11356-014-3265-1.

Ben Ameer, W., Trabelsi, S., Megdiche, Y., Ben Hassine, S., Barhoumi, B., Hammami, B., Eljarrat, E., Barceló, D., Ridha Driss, M., 2013. Concentration of polychlorinated biphenyls and organochlorine pesticides in mullet (*Mugil cephalus*) and sea bass (*Dicentrarchus labrax*) from Bizerte Lagoon (Northern Tunisia). *Chemosphere* 90, 2372–2380.

Ben Ismail, C., Sammari, G.P., Béranger, Gasparini K., Brahim, M., Aleya, L., 2012. Water masses exchanged through the channel of Sicily: evidence for the presence of new water masses on the Tunisian side of the channel. *Deep-Sea Res.* 1 63, 65–81.

Ben Ismail, S., Schröder, K., Sammari, C., Gasparini, G.P., Borghini, M., Aleya, L., 2014. Interannual variability of water mass properties in the Tunisia-Sicily channel. *J. Marine Syst.* 135, 14–28.

Bonneville, S., Smits, M.M., Brown, A., Harrington, J., Leake, J.R., Brydson, R., Benning, L.G., 2009. Plant-driven fungal weathering: early stages of mineral alteration at the nanometer scale. *Geology* 37, 615–618.

D'Errico, G., Giovannelli, D., Montano, C., Milanovic, V., Ciani, M., Manini, E., 2013. Bioremediation of high organic load lagoon sediments: compost addition and priming effects. *Chemosphere* 91, 99–104.

Eijsink, L.M., Krom, M.D., De Lange, G.J., 1997. The use of sequential extraction techniques for sedimentary phosphorus in eastern Mediterranean sediments. *Mar. Geol.* 139, 147–155.

Eijsink, L.M., Krom, M.D., Herut, B., 2000. Speciation and burial flux of phosphorus in the surface sediments of the eastern Mediterranean. *Am. J. Sci.* 300, 483–503.

Fertouna-Bellakhal, M., Dhib Béjaoui, A., Turki, S., Aleya, L., 2014. Driving factors behind the distribution of dinocyst composition and abundance in surface sediments in a western Mediterranean coastal lagoon: report from a high resolution mapping study. *Mar. Pollut. Bull.* 84, 347–362.

Gomez, E., Durillon, C., Rofes, G., Picot, B., 1999. Phosphate adsorption and release from sediments of brackish lagoons: pH, O₂ and loading influence. *Water Res.* 33, 2437–2447.

Jilbert, T., Reichert, G.-J., Aeschlimann, B., Günther, D., Boer, W., De Lange, G., 2010. Climate-controlled multidecadal variability in North African dust transport to the Mediterranean. *Geology* 38, 19–22.

Koroleff, F., 1976. Determination of nutrients. In: Grasshoff, K., et al. (Ed.), *Methods of seawater analysis*. 2nd Ed. Verlag-Chemie, pp. 156–117.

Kraal, P., Slomp, C.P., De Lange, G.J., 2010. Sedimentary organic carbon to phosphorus ratios as a redox proxy in quaternary records from the Mediterranean. *Chem. Geol.* 277, 167–177.

Krom, M.D., Berner, R.A., 1980. Adsorption of phosphate in anoxic marine sediments. *Limnol. Oceanogr.* 25, 797–806.

Krom, M.D., Groom, S., Zohary, T., 2003. The eastern Mediterranean. In: Black, K.D., Shimmield, G.B. (Eds.), *The Biogeochemistry of Marine Systems*. Blackwell Publishing, Oxford, pp. 91–122.

Krom, M.D., Emeis, K.C., Van Cappellen, P., 2010. Why is the eastern Mediterranean phosphorus limited? *Prog. Oceanogr.* 85, 236–244.

Kuster-Heins, K., Steinmetz, E., De Lange, G.L., Zabel, M., 2010. Phosphorus cycling in marine sediments from the continental margin off Namibia. *Mar. Geol.* 274, 95–106.

Lucas, J., Prévôt, L., 1984. Synthèse de l'apatite par voie bactérienne à partir de matière organique phosphatée et de divers carbonates de calcium dans des eaux douces et marines naturelles. *Chem. Geol.* 42, 101–118.

- Lucotte, M., D'Anglejan, B., 1985. A comparison of several methods for the determination of iron hydroxides and associated orthophosphates in estuarine particulate matter. *Chem. Geol.* 48, 257–264.
- Nowacka, B., Stone, A.T., 2006. Competitive adsorption of phosphate and phosphonates on to goethite. *Water Res.* 40, 2201–2209.
- Paytan, A., Mc Laughlin, K., 2007. The oceanic phosphorus cycle. *Chem. Rev.* 107, 563–576.
- Poulton, S.W., Canfield, D.E., 2006. Co-diagenesis of iron and phosphorus in hydrothermal sediments from the southern east Pacific Rise; implications for the evaluation of paleo-sea water phosphate concentrations. *Geochim. Cosmochim. Acta* 70, 5883–5898.
- Ruttenberg, K.C., 1992. Development of a sequential extraction method for different forms of phosphorus in marine sediments. *Limnol. Oceanogr.* 37, 1460–1482.
- Sahraoui, I., Sakka, H.A., Hadj, M.H., Leger, C., Bates, S.S., 2009. Blooms of the diatoms genus *Pseudo-nitzschia* H. Peragallo in Bizerte lagoon (Tunisia, SW Mediterranean). *Diatom Res.* 24, 175–190.
- Slomp C.P., 2011. Phosphorus Cycling in the Estuarine and Coastal Zones: Sources, Sinks, and Transformations. In: Wolanski E and McLusky DS (Eds.) *Treatise on Estuarine and Coastal Science*, 5, 201–229.
- Smida, D.B., Sahraoui, I., Hadj, M.H., Sakka, H.A., 2012. Dynamique saisonnière du genre *Alexandrium* (dinoflagellé potentiellement toxique) dans la lagune de Bizerte (Nord de la Tunisie) et contrôle par les facteurs abiotiques environnants. *C.R. Biol.* 335, 406–416.
- Tang, C.M., Stott, L.D., 1993. Seasonal salinity changes during Mediterranean sapropel deposition 9000 years B.P: evidence from isotopic analyses of individual planktonic foraminifera. *Paleoceanography* 8, 473–493.
- Thouvenot-Korppoo, M., Lukkari, K., Järvelä, J., Leivuori, M., Karvonen, T., Stipa, T., 2012. Phosphorus release and sediment geochemistry in a low-salinity water bay of the Gulf of Finland. *Boreal Environ. Res.* 17, 237–251.
- Turki, S., Dhib, A., Belakhal, M.F., Frossard, V., Balti, N., Kharrat, R., Aleya, L., 2014. What can be learned from a five-year monitoring of harmful algal blooms associated with phycotoxins in a Mediterranean lagoon? *Ecol. Eng.* 67, 39–47.
- Van der Heide, T., Smolders, A.J.P., Lamers, L.P.M., Van Katwijk, M.M., Roelofs, J.G.M., 2010. Nutrient availability correlates with bicarbonate accumulation in marine and freshwater sediments—empirical evidence from pore water analyses. *Appl. Geochem.* 25, 1825–1829.
- Watanabe, F.S., Olsen, S.R., 1962. Colorimetric determination of phosphorus in water extracts of soils. *Soil Sci.* 93, 183–188.
- Zabel, M., Dahmke, A., Schulz, H.D., 1998. Regional distribution of diffusive phosphate and silicate fluxes through the sediment–water interface: the eastern South Atlantic. *Deep-Sea Res.* 45, 277–300.